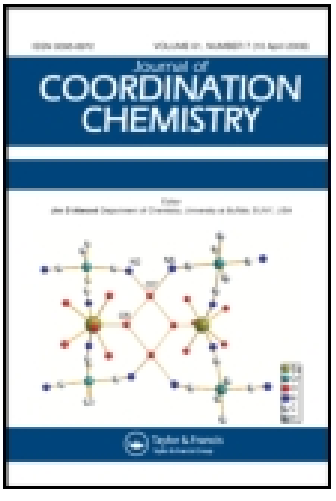


Journal of Coordination Chemistry
Publication details, including instructions for authors and subscription information:
http://www.tandfonline.com/loi/gcoo20

# Binuclear transition metal complexes of bicompartmental SNO donor ligands: synthesis, characterization, and electrochemistry

Naveen V. Kulkarni [a], M.P. Sathisha [a], Srinivasa Budagumpi [a], Gurunath S. Kurdekar [a] & Vidyanand K. Revankar [a]
[a] Department of Studies in Chemistry, Karnatak University, Pavate Nagar, Dharwad 580 003, Karnataka, India
Published online: 09 Apr 2010.

To cite this article: Naveen V. Kulkarni, M.P. Sathisha, Srinivasa Budagumpi, Gurunath S. Kurdekar & Vidyanand K. Revankar (2010) Binuclear transition metal complexes of bicompartmental SNO donor ligands: synthesis, characterization, and electrochemistry, Journal of Coordination Chemistry, 63:8, 1451-1461, DOI: 10.1080/00958971003770405

To link to this article: http://dx.doi.org/10.1080/00958971003770405

*Journal of Coordination Chemistry*
Vol. 63, No. 8, 20 April 2010, 1451–1461



# Binuclear transition metal complexes of bicompartmental SNO donor ligands: synthesis, characterization, and electrochemistry

NAVEEN V. KULKARNI, M.P. SATHISHA, SRINIVASA BUDAGUMPI, GURUNATH S. KURDEKAR and VIDYANAND K. REVANKAR*

Department of Studies in Chemistry, Karnatak University, Pavate Nagar, Dharwad 580 003, Karnataka, India

(*Received 4 October 2009; in final form 23 December 2009*)

A series of new binucleating $Co^{II}$, $Ni^{II}$, $Cu^{II}$, and $Zn^{II}$ complexes of bicompartmental ligands with SNO donors was prepared. The Schiff bases were obtained by the condensation of 4,6-diacetylresorcinol and mercapto-substituted 1,2,4-triazoles. The ligands and their complexes were characterized by elemental analysis, infrared, $^1$H-NMR, UV-Vis, FAB-mass, and ESR spectral studies, magnetic susceptibility, and conductivity measurements. All the complexes were monomeric and binuclear. $Ni^{II}$ and $Co^{II}$ complexes were octahedral, whereas $Cu^{II}$ and $Zn^{II}$ complexes were square planar and tetrahedral, respectively. The compounds are investigated for electrochemical activity.

*Keywords*: 4,6-Diacetylresorcinol; Triazole; Schiff base; Binuclear complex



## 1. Introduction

Synthesis of binuclear complexes in which a ligand structure maintains two metal centers in close proximity but in different compartments separated by an intervening group represents an important current objective in transition-metal systems. These complexes serve as simple models for multi-metal-centered catalysts and multielectron-transfer reagents [1–4]. The orientation of the metal centers, and hence the nature of the metal–metal interactions, are controlled *via* appropriate bridging ligands [5, 6]. The bifunctional carbonyl compound, 4,6-diacetylresorcinol, serves as precursor for the formation of different polydentate ligands [7–11] and as primary ligand in the various mixed-ligand complexes [12, 13]. 4,6-Diacetylresorcinol is also employed in the construction of SNO chelating ligands by the condensation of thiosemicarbazides [14] and thiocarbohydrazide [15]. These ligands are employed to synthesize mono-, bi-, and poly-nuclear complexes with different binding modes and the structural and functional features were explored.

*Corresponding author. Email: vkrevankar@rediffmail.com

*Journal of Coordination Chemistry*
ISSN 0095-8972 print/ISSN 1029-0389 online 
DOI: 10.1080/00958971003770405

In this study, 4,6-diacetylresorcinol is selected as precursor for the construction of bicompartmental ligands. The two carbonyl groups at the 4- and 6-positions are expected to form Schiff bases with amines and the adjacent hydroxy groups may construct two coordination compartments with the help of azomethine nitrogen and other functionalities present in amines. The aromatic ring acts as a bridge as well as a rigid separator between the two compartments.

Amine- and mercapto-substituted triazoles have versatile coordination behavior toward transition metal ions by providing several monodentate binding modes and SN bidentate coordination through S=C–NH–$NH_2$, which results in an enormous number of complexes [5, 16]. Incorporation of an additional coordinating functionality to the amino-mercapto triazoles *via* Schiff base formation generates a group of multidentate organic hosts with considerable coordination potential. These undergo chelation with transition metal ions and exhibit versatile stereo- and electro-chemical properties [17, 18]. To utilize these features, amino-mercapto-substituted triazoles are employed for the construction of bicompartmental SNO donors.

Complexes of SNO donors have versatile structural and functional properties and applications in the field of biochemistry and catalysis [19–21]. Construction of bicompartmental SNO donor ligands and their complexes is, hence, of interest. The rigid aromatic spacer separates the two cavities and avoids the possibility of direct spin–spin interaction between metal centers. Therefore, the direct influence of one metal site on the steric and electronic properties of another is avoided, making the structural and functional properties interesting.



## 2. Experimental

### 2.1. *Materials and methods*

The chemicals used were of reagent grade and the solvents were dried and distilled before use according to standard procedures; 3-methyl-5-mercapto-4-amino-1,2,4-triazole (MMAT), 3-methylsulfhydryl-4-amino-5-mercapto-1,2,4-triazole (MAMT) [22], and 4,6-diacetylresorcinol [23] were synthesized according to the methods in literature. The metal chlorides used were in the hydrated form. Elemental analysis was carried out on a Thermo quest elemental analyzer; metal and chloride analyses were done by following standard procedures. The molar conductivity measurements in dimethylformamide (DMF) were made on an ELICO-CM-82 conductivity bridge with conductivity cell having cell constant 0.51 $cm^{-1}$. The numerical details of elemental analysis and conductivity measurements are shown in table 1. Magnetic susceptibility measurements were made using a Faraday balance at room temperature using $Hg[Co(SCN)_4]$ as calibrant. $^1$H-NMR spectra were recorded in DMSO-$d_6$ on a Bruker-300 MHz spectrometer at room temperature using TMS as internal reference. IR spectra were recorded in KBr using an Impact-410 Nicolet (USA) FT-IR spectrometer from 4000 to 400 $cm^{-1}$. Electronic spectra of the complexes in DMF were recorded on a Hitachi 150-20 spectrophotometer in the range 1000–200 nm. Cyclic voltammetric studies were performed at room temperature in DMF under oxygen-free conditions created by purging pure nitrogen gas with a CHI1110A electrochemical analyzer (USA) comprising a three electrode assembly of glassy carbon working

Table 1. Chemical composition and molar conductivity data.

| Compound | Yield (%) | Color | Melting point (°C) | Elemental analysis found (calculated) (%) | | | | | | Molar conductivity, $\Lambda_m$ ($ohm^{-1}\,cm^2\,mol^{-1}$) |
|---|---|---|---|---|---|---|---|---|---|---|
| | | | | C | H | N | S | M | Cl | |
| $L^1H_4$ | 82 | Colorless | 180–182 | 45.98 (45.93) | 4.38 (4.30) | 26.84 (26.79) | 15.43 (15.31) | – | – | – |
| $[Co_2L^1(H_2O)_6]\cdot H_2O$ | 76 | Pink | >280 | 29.24 (29.18) | 4.32 (4.25) | 17.12 (17.02) | 9.89 (9.72) | 18.12 (17.90) | – | 6.2 |
| $[Ni_2L^1(H_2O)_6]\cdot H_2O$ | 78 | Light green | >280 | 29.28 (29.21) | 4.38 (4.26) | 17.16 (17.04) | 9.79 (9.73) | 18.03 (17.83) | – | 8.4 |
| $[Cu_2L^1(H_2O)_2]\cdot H_2O$ | 76 | Brown | >280 | 32.29 (32.21) | 3.42 (3.36) | 18.97 (18.81) | 10.93 (10.75) | 21.53 (21.34) | – | 10.1 |
| $[Zn_2L^1H_2Cl_2]\cdot H_2O$ | 74 | Colorless | >280 | 30.38 (30.30) | 2.87 (2.82) | 17.68 (17.52) | 10.15 (10.11) | 21.16 (20.67) | 11.36 (11.06) | 7.3 |
| $L^2H_4$ | 80 | Colorless | 198–200 | 39.91 (39.83) | 3.86 (3.73) | 23.29 (23.24) | 26.63 (26.5) | – | – | – |
| $[Co_2L^2H_2Cl_2(H_2O)_4]\cdot 2H_2O$ | 78 | Pink | >280 | 26.10 (26.02) | 3.12 (2.98) | 15.22 (15.18) | 17.41 (17.34) | 16.08 (15.96) | 10.12 (9.53) | 7.4 |
| $[Ni_2L^2H_2Cl_2(H_2O)_4]\cdot 2H_2O$ | 75 | Light green | >280 | 26.14 (26.06) | 3.09 (3.02) | 15.31 (15.22) | 17.45 (17.37) | 16.01 (15.89) | 10.02 (9.49) | 6.5 |
| $[Cu_2L^2(H_2O)_2]$ | 78 | Brown | >280 | 29.93 (29.86) | 2.86 (2.79) | 17.53 (17.41) | 19.98 (19.90) | 20.03 (19.75) | – | 8.7 |
| $[Zn_2L^2H_2Cl_2]\cdot 2H_2O$ | 75 | Colorless | >280 | 26.46 (26.40) | 2.84 (2.75) | 15.54 (15.45) | 17.81 (17.66) | 18.43 (18.04) | 10.24 (9.65) | 5.3 |

electrode, platinum auxiliary electrode, and $Ag^{+}/AgCl$ reference electrode. Tetramethylammoniumchloride (0.1 mol $dm^{-3}$) was used as supporting electrolyte and the instrument was standardized by ferrocene/ferrocenium redox couple. ESR study of the copper complexes was carried out on a Varian E-4X-band EPR spectrometer with field intensity at ~3000 G, using TCNE as the g-marker. FAB mass spectra were recorded on a JEOL SX 102/DA-6000 mass spectrometer using Argon/Xenon (6 kV, 10 mA) as the FAB gas and 3-nitrobenzylalcohol as matrix. TG analysis of the complexes was done in nitrogen on a Universal V2 4F TA instrument at 10 °C $min^{-1}$ and scan range of 25–800°C.



### 2.2. *General procedure for the preparation of ligands*

Hot solution of triazole (0.02 mol, 2.68 g (MMAT) or 3.32 g (MAMT) in 100 mL of methanol was treated with methanolic solution of 4,6-diacetylresorcinol (0.01 mol, 1.94 g). The mixture was stirred and refluxed for 4–5 h on a steam bath. The solid product was filtered, washed with methanol, and dried over anhydrous $CaCl_2$. The reaction pathway is represented in figure 1.

### 2.3. *General procedure for the preparation of complexes*

Metal(II) chloride {$CoCl_2 \cdot 6H_2O$ (0.475 g, 0.002 mol), $NiCl_2 \cdot 6H_2O$ (0.474 g, 0.002 mol), $CuCl_2 \cdot 2H_2O$ (0.341 g, 0.002 mol), and $ZnCl_2$ (0.271 g, 0.002 mol)} in methanol was added with stirring to 50 mL of methanolic solution (0.001 mol) of $L^1H_4$ (0.294 g) or $L^2H_4$ (0.326 g, 0.001 mol). The mixture was then refluxed for 2 h on a water bath; the obtained complexes were filtered off and dried over anhydrous $CaCl_2$.

## 3. Results and discussion

### 3.1. *Molar conductivity measurements*

The molar conductance values of the complexes measured at room temperature in DMSO solution at $10^{-3}$ mol $dm^{-3}$ were in the range 5.3–10.1 ohm$^{-1}$ $cm^2$ $mol^{-1}$, indicating non-electrolytic nature for the complexes.

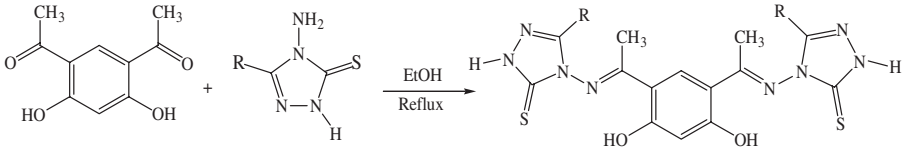


Figure 1. Schematic representation of the preparation of ligands.

### 3.2. *Infrared spectral studies*

IR spectra of the free ligands show a band of medium intensity at 3140–3290 $cm^{-1}$ assigned to $\nu$(NH). The absence of a band at 2400–2600 $cm^{-1}$ due to $\nu$(SH) in $L^1H_4$ and $L^2H_4$ confirms that the ligands exist in the thioketo form. The sharp band around 1630 $cm^{-1}$ assigned to $\nu$(C=N) in the free ligands shifts to lower frequency in spectra of the complexes, suggesting the coordination of both azomethine nitrogens to the metal. The broad $\nu$(O–H) at ~3400 $cm^{-1}$ in the free ligands is absent in spectra of all the complexes except $[Zn_2L^1H_2Cl_2]\cdot H_2O$, suggesting deprotonation of the phenolic oxygen on coordination. The vibrational couplings among thioamide group are around 1550, 1450, 1320, and 975 $cm^{-1}$. In $[Co_2L^2H_2Cl_2(H_2O)_4]\cdot 2H_2O$, $[Ni_2L^2H_2Cl_2(H_2O)_4]\cdot 2H_2O$, and $[Zn_2L^2H_2Cl_2]\cdot 2H_2O$ the signal due to $\nu$(NH) is retained and thioamide bands which have major contribution of $\nu$(C=S) are reduced in intensity, which supports the thioketo mode [18] of coordination of sulfur. In all other complexes no thioamide bands indicates thioenolization and subsequent coordination to metal, which is supported by the appearance of a weak band at 670 $cm^{-1}$ due to $\nu$(C–S) and disappearance of $\nu$(N–H). The sulfhydryl $\nu$(SH) in $L^2H_4$ at 2600 $cm^{-1}$ is further confirmed by a signal at 5.4 ppm in $^1$H-NMR spectrum. Generally $-CH_2SH$ is a good coordinating site, but in the present case the non-participation of $-CH_2SH$ in coordination may be due to the presence of stronger coordinating mercapto- and thioketo-group, suppressing $-CH_2SH$ coordination [18]. Further, the possibility of $-CH_2SH$ acting as an additional binding site to the metal is ruled out due to steric constraints which may affect complex formation. The low-frequency bands at 500–465 and 440–410 $cm^{-1}$ are assigned to $\nu$(M–N) and $\nu$(M–S), respectively. All the complexes exhibit a broad peak at 3400 $cm^{-1}$ suggesting the presence of coordinated water. The IR spectral data are given in table 2.

### 3.3. *$^1$H-NMR studies*

Proton-NMR data for the ligands and binuclear $Zn^{II}$ complexes were recorded. In spectra of ligands, the signals around 12.80 and 14.00 ppm are assigned to –OH and –NH of diacetophenone and triazole. For $[Zn_2L^1H_2Cl_2]\cdot H_2O$, phenolic –OH is retained, but the –NH signal disappears on complexation, owing to the thioenolization followed by deprotonation. Resonance due to the methyl attached to the triazole ring at 2.4 ppm in $L^1H_4$ remains unaltered in the complex. In $[Zn_2L^2H_2Cl_2]\cdot 2H_2O$, disappearance of signal at 12.80 ppm indicates chelation of the ligand accompanied with the deprotonation of phenolic –OH [24]. The retention of signal corresponding to –NH ($D_2O$ exchangeable) in the spectrum suggest that the complexation is *via* thioketo sulfur. Resonance due to sulfhydryl –SH in $L^2H_4$, which appears at 5.48 ppm ($D_2O$ exchangeable) and the methylene group attached to –SH group identified at 3.90 ppm are also retained in the complex. Further, the methyl of acetyl and the diacetophenone ring protons are at 2.60 and 6.00–8.00 ppm, respectively, in both ligands and their corresponding complexes. A considerable degree of symmetry is present in these compounds so that the protons in the two halves of the molecules are magnetically equivalent. Relative to the free ligands, the dizinc complexes show small shift in proton resonance frequencies, attributable to variation in electron density and steric constraints brought about in the compounds upon complexation [24].

Table 2. Infrared spectral data of ligands and complexes in $cm^{-1}$.

| Compound | ν(N–H) triazole | ν(C=N) azomethine | ν(C=S) thioamidic | | ν(C–S) | ν(S–H) | ν(O–H)phenolic | ν(C–O) | ν(M–N) | ν(M–S) |
|---|---|---|---|---|---|---|---|---|---|---|
| $L^1H_4$ | 3292 | 1632 | 1240 | 746 | – | – | 3060 | 1375 | – | – |
| $[Co_2L^1(H_2O)_6]\cdot H_2O$ | 3200 | 1617 | – | – | 665 | – | – | 1368 | 478 | 416 |
| $[Ni_2L^1(H_2O)_6]\cdot H_2O$ | 3213 | 1619 | – | – | 667 | – | – | 1350 | 470 | 410 |
| $[Cu_2L^1(H_2O)_2]\cdot H_2O$ | 3303 | 1620 | – | – | 675 | – | – | 1372 | 472 | 418 |
| $[Zn_2L^1H_2Cl_2]\cdot H_2O$ | 3229 | 1617 | – | – | 697 | – | 3010 | 1372 | 471 | 414 |
| $L^2H_4$ | 3295 | 1631 | 1252 | 755 | – | 2450 | 3058 | 1326 | – | – |
| $[Co_2L^2H_2Cl_2(H_2O)_4]\cdot 2H_2O$ | 3277 | 1620 | 1230 | 774 | – | 2420 | – | 1390 | 474 | 430 |
| $[Ni_2L^2H_2Cl_2(H_2O)_4]\cdot 2H_2O$ | 3196 | 1618 | 1241 | 730 | – | 2400 | – | 1398 | 490 | 425 |
| $[Cu_2L^2(H_2O)_2]$ | 3200 | 1627 | – | – | 658 | 2410 | – | 1399 | 470 | 426 |
| $[Zn_2L^2H_2Cl_2]\cdot 2H_2O$ | 3222 | 1617 | 1232 | 780 | – | 2440 | – | 1377 | 476 | 440 |

### 3.4. *Magnetic properties, electronic, and EPR spectral studies*

Electronic spectra of the ligands in DMF show bands in the range 275–345 nm. The higher energy bands in the region 275–290 nm are assigned to $\pi$–$\pi^*$ transitions of the aromatic ring. The medium energy bands in the region 290–330 nm are assigned to $n$–$\pi^*$ transitions of the azomethine nitrogen and thione sulfur. Lower energy bands with molar extinction coefficient $\varepsilon \sim 25{,}000\ \mathrm{L\,cm^{-1}\,mol^{-1}}$ at 330–345 nm are attributed to intraligand charge transfer (CT) transitions [25]. The UV-Vis spectra of $Cu^{II}$ complexes in DMF have bands around 400 nm with $\varepsilon \sim 25{,}000\ \mathrm{L\ cm^{-1}\,mol^{-1}}$ and 600 nm with $\varepsilon \sim 300\ \mathrm{L\,cm^{-1}\,mol^{-1}}$ attributable to CT transition of $S \rightarrow Cu^{II}$ [18] and the d–d transition, $^2B_{1g} \rightarrow {}^2E_{2g}$, $d_{x^2-y^2} \rightarrow d_{z^2}$ corresponding to square-planar structure [26]. The magnetic moments of 1.84 and 1.86 BM, respectively, above the spin-only value for $Cu^{II}$ suggest square-planar structure for the complex [27]. The broad isotropic peak observed with $g_{iso}$ 2.01 and 2.03 in the X-band EPR spectra suggest the absence of spin–spin interaction in the complexes. In the electronic spectra of nickel complexes three d–d bands were observed at 840, 520, and 450 nm with $\varepsilon \sim 300\ \mathrm{L\,cm^{-1}\,mol^{-1}}$ attributable to spin-allowed transitions $^3A_{2g} \rightarrow {}^3T_{2g}$, $^3A_{2g} \rightarrow {}^3T_{1g}$, and $^3A_{2g} \rightarrow {}^3T_{1g}(P)$, respectively, representing octahedral complex [25]; the magnetic moments (3.18 and 3.24 BM) obtained for both complexes suggest the same [28]. The octahedral $Co^{II}$ complexes usually show three bands [26], but in the present case only one peak corresponding to $^4T_{1g}(F) \rightarrow {}^4T_{1g}(P)$ was observed at 500 nm ($\varepsilon \sim 300\ \mathrm{L\,cm^{-1}\,mol^{-1}}$) in both cobalt complexes due to the fact that the band due to $^4T_{1g}(F) \rightarrow {}^4T_{2g}$ occurs in near infrared region and the band due to $^4T_{1g} \rightarrow {}^4A_{2g}$ involves a two-electron transition. Octahedral geometry was assigned to the complexes by considering the magnetic moment values 4.20 and 4.26 BM, respectively [28, 29]. The diamagnetic zinc complexes show absorptions only in the higher frequency region with high extension coefficient values attributed to the ligand electron transitions.

### 3.5. *FAB mass spectral studies*

FAB mass spectral studies provide supporting evidence for the proposed constitutions of the complexes (represented in figure 2). The two copper complexes selected as representative show the molecular ion peaks at $m/z$ 599 and $m/z$ 643 that correspond to the formula weight $[Cu_2L^1(H_2O)_2] \cdot H_2O$ and $[Cu_2L^2(H_2O)_2]$, respectively, for binuclear monomeric complexes.

### 3.6. *Thermogravimetric analysis*

The thermal stability and decomposition pattern of the complexes were analyzed by thermogravimetric studies under nitrogen with a heating rate of $10^\circ\mathrm{C\,min^{-1}}$. Decomposition of $[Cu_2L^1(H_2O)_2] \cdot H_2O$ takes place in three stages. The first stage corresponds to a mass loss of ~2.8% around 91°C, attributed to the elimination of solvated water. The second stage of a mass loss of 6.62% taking place at 185°C corresponds to the loss of two coordinated water molecules. Further reduction of mass in a higher temperature range (around 250°C) is ascribed to ligand decomposition. The final product was metal-oxide. The copper complex $[Cu_2L^2(H_2O)_2]$ also exhibits three-step decomposition pattern with 6.67% weight loss at 150°C corresponding to the

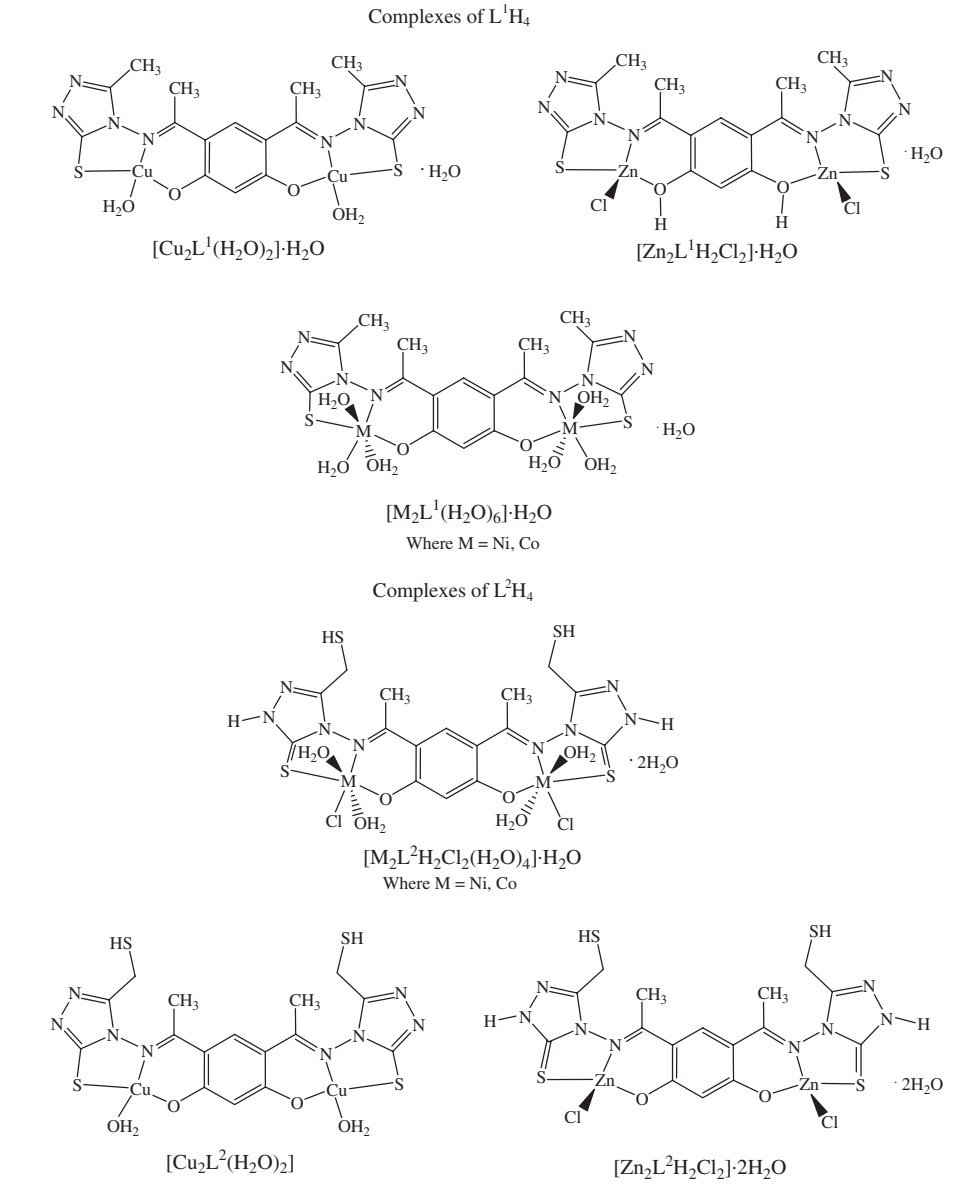


Figure 2. Proposed structures of complexes $[L^1H_4]$ and $[L^2H_4]$.

elimination of two water molecules. The weight loss of 7.02% and 25.57% observed around 200°C and 350°C is attributed to the decomposition of ligand.

### 3.7. *Electrochemical measurements*

The cyclic voltammetric study of ligands and complexes in DMSO (0.001 mol) was carried out in the potential range of −0.1 to 1.0 V in $O_2$ free condition with different

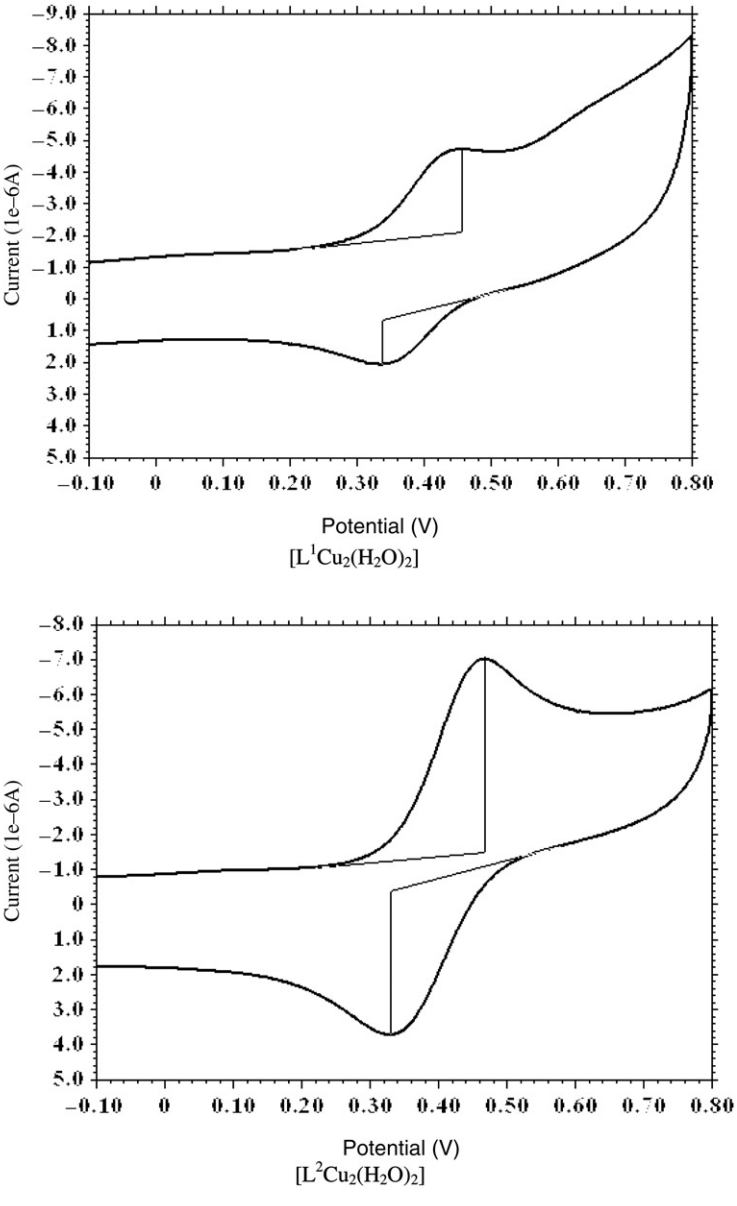


Figure 3. Cyclic voltammograms of copper complexes at scan rate of $0.1\,V\,s^{-1}$.

scan rates (0.15, 0.1, and $0.05\,V\,s^{-1}$). Only the copper complexes exhibited redox properties. This suggests that the electrochemical activity of the copper complexes is purely based on metal.

The voltammograms of the two copper complexes are shown in figure 3 and numerical results are given in table 3. In the electrochemical investigation of $[Cu_2L^1(H_2O)_2]\cdot H_2O$ anodic peak ($E_{pa}$) observed in the voltammogram in the potential range 0.44–0.46 V represents oxidation ($Cu^{II} \rightarrow Cu^{III}$). The corresponding cathodic

Table 3. Cyclic voltammetry results.

| Complex | Scan rate ($V\,s^{-1}$) | $E_{pa}$ (V) | $E_{pc}$ (V) | $\Delta E_p$ (V) | $E_{1/2}$ (V) | $I_{pc}/I_{pa}$ |
|---|---|---|---|---|---|---|
| $[Cu_2L^1(H_2O)_2]\cdot H_2O$ | 0.15 | 0.46 | 0.34 | 0.12 | 0.40 | 0.72 |
| | 0.1 | 0.45 | 0.35 | 0.10 | 0.40 | 0.74 |
| | 0.05 | 0.44 | 0.36 | 0.08 | 0.40 | 0.77 |
| $[Cu_2L^2(H_2O)_2]$ | 0.15 | 0.47 | 0.32 | 0.15 | 0.39 | 0.73 |
| | 0.1 | 0.46 | 0.33 | 0.13 | 0.39 | 0.75 |
| | 0.05 | 0.43 | 0.34 | 0.09 | 0.38 | 0.78 |

$\Delta E_p = E_{pa} - E_{pc}$ and $E_{1/2} = [E_{pc} + E_{pa}]/2$.



potential scan gives a peak ($E_{pc}$) with potential in the range 0.34–0.36 V representing reduction ($Cu^{III} \rightarrow Cu^{II}$). $[Cu_2L^2(H_2O)_2]$ shows similar behavior, with corresponding anodic peak, $E_{pa}$, in the range 0.43–0.47 V and cathodic peak, $E_{pc}$, in the range 0.32–0.34. The high value of $\Delta E_p$, separation between the cathodic and anodic peak potentials ($E_{pa} - E_{pc}$), in both cases greater than 60 mV (which varies with scan rate), indicates quasi-reversible nature of the redox process [30, 31].

## 4. Conclusion

$L^1H_4$ is hexadentate tetrabasic for $Co^{II}$, $Ni^{II}$, and $Cu^{II}$ complexes and hexadentate dibasic chelate for $Zn^{II}$. On the other hand, $L^2H_4$ is hexadentate tetrabasic for $Cu^{II}$ and hexadentate dibasic in other complexes. Both ligands provide SNO donating sites to each metal ion in the binuclear complexes. $Cu^{II}$ and $Zn^{II}$ complexes of both ligands have square-planar and tetrahedral geometry, respectively, whereas $Co^{II}$ and $Ni^{II}$ complexes are octahedral. The $Cu^{II}$ complexes exhibit quasi-reversible redox activity in the applied potential range. Further studies are necessary to understand catalytic behavior and multielectron-transfer mechanism of compounds.

## Acknowledgements

The authors thank the Department of Chemistry and USIC, Karnatak University, Dharwad, for providing spectral and analytical facility. Recording of FAB mass spectra (CDRI, Lucknow) and ESR spectra (IIT, Bombay) are gratefully acknowledged. N.V. Kulkarni and M.P. Satisha thank Karnatak University, Dharwad, for providing the Nilekani and University Research Scholarship, and S. Budagumpi thanks the University Grant Commission for providing RFSMS.

## References

[1] L.V. Penkova, A. Maciag, E.V. Rybak-Akimova, M. Haukka, V.A. Pavlenko, T.S. Iskenderov, H. Kozlowski, F. Meyer, I.O. Fritsky. *Inorg. Chem.*, **48**, 6960 (2009).
[2] C. Camacho-Camacho, G. Merino. *Eur. J. Inorg. Chem.*, 1021 (1999).

[3] F.R. Keene, J.A. Smith, J.G. Collins. *Coord. Chem. Rev.*, **253**, 2021 (2009).
[4] S.J. Lippard, J.M. Berg. *Principles of Bioinorganic Chemistry*, University Science Books, Mill Valley, CA (1994).
[5] K. Singh, Dharampal, V. Parkash. *Phosphorus, Sulfur Silicon Relat. Elem.*, **183**, 2784 (2008).
[6] P. Chaudhuri, V. Kataev, B. Buchner, H.-H. Klauss, B. Kersting, F. Meyer. *Coord. Chem. Rev.*, **253**, 2261 (2009).
[7] U.B. Gangadharmath, V.K. Revankar, V.B. Mahale. *Spectrochim. Acta, Part A*, **58**, 2651 (2002).
[8] H.S. Seleem, B.A. El-Shetary, S.M.E. Khalil, M. Mostafa, M. Shebl. *J. Coord. Chem.*, **58**, 479 (2005).
[9] A.A.A. Emara, A.A.A. Abou-Hussen. *Spectrochim. Acta, Part A*, **64**, 1010 (2006).
[10] A.A.A. Abou-Hussen. *J. Coord. Chem.*, **59**, 157 (2006).
[11] M. Shebl. *Spectrochim. Acta, Part A*, **73**, 313 (2009).
[12] A. Taha. *Spectrochim. Acta, Part A*, **59**, 1611 (2003).
[13] S.-L. Liu, C.-L. Wen, S.-S. Qi, E.-X. Liang. *Spectrochim. Acta, Part A*, **69**, 664 (2008).
[14] H.S. Seleem, A.A. Emara, M. Shebl. *J. Coord. Chem.*, **58**, 1003 (2005).
[15] H.S. Seleem, B.A. El-Shetary, M. Shebl. *Heteroatom. Chem.*, **18**, 100 (2007).
[16] V.B. Badwaik, A.S. Aswar. *Russian J. Coord. Chem.*, **33**, 10755 (2007).
[17] M. Cingi, F. Bigoli, M. Lanfranchi, E. Leporati, M. Pellinghelli, C. Fogua. *Inorg. Chim. Acta*, **235**, 37 (1995).
[18] A.D. Naik, S.M. Annigeri, U.B. Gnagadharmath, V.K. Revankar, V.B. Mahale, V.K. Reddy. *Indian J. Chem.*, **41A**, 2046 (2002).
[19] M. Sönmez, M.R. Bayram, M. Çeleb. *J. Coord. Chem.*, **62**, 2728 (2009).
[20] A. Rana, M. Sutradhar, S.S. Mandal, S. Ghosh. *J. Coord. Chem.*, **62**, 3522 (2009).
[21] N.R. Pramanik, S. Ghosh, T.K. Raychaudhuri, S.S. Mandal. *J. Coord. Chem.*, **62**, 3845 (2009).
[22] K.S. Dhaka, J. Mohan, V.K. Chadda, H.K. Pujari. *Indian J. Chem.*, **12**, 287 (1974).
[23] M. Zheng, S.V. Khanyubv, G.C. Dismukes, V.V. Barynin. *Inorg. Chem.*, **33**, 382 (1994).
[24] R.M. Issa, S.A. Azim, A.M. Khedr, D.F. Draz. *J. Coord. Chem.*, **62**, 1859 (2009).
[25] A.B.P. Lever. *Inorganic Electronic Spectroscopy*, Elsevier Publishing Company, New York (1968).
[26] A.A.A. Abu-Hussen, W. Linert. *J. Coord. Chem.*, **62**, 1388 (2009).
[27] M.P. Sathisha, V.K. Revankar. *J. Coord. Chem.*, **62**, 2540 (2009).
[28] K.S. Abou-Melha. *J. Coord. Chem.*, **61**, 2053 (2008).
[29] S.B. Kalia, K. Lumba, G. Kaushal, M. Sharma. *Indian J. Chem.*, **46A**, 1233 (2007).
[30] C.L. Bailey, R.D. Bereman, D.P. Rillema. *Inorg. Chem.*, **25**, 3149 (1986).
[31] N. Raman, S. Johnson Raja, A. Sakthivel. *J. Coord. Chem.*, **62**, 691 (2009).